

One-body dissipation and chaotic dynamics in a classical simulation of a nuclear gas

M. Baldo, G. F. Burgio, and A. Rapisarda

*Istituto Nazionale di Fisica Nucleare, Sezione di Catania and Dipartimento di Fisica, Università di Catania,
Corso Italia 57, I-95129 Catania, Italy*

P. Schuck

Institut de Physique Nucléaire, Université de Grenoble, 53 Avenue des Martyrs, 38026 Grenoble Cedex, France

(Received 31 July 1998)

In order to understand the origin of one-body dissipation in nuclei, we analyze the behavior of a gas of classical particles moving in a two-dimensional cavity with nuclear dimensions. This “nuclear” billiard has multipole-deformed walls which undergo periodic shape oscillations. We demonstrate that a single-particle Hamiltonian containing coupling terms between the particle motion and the collective coordinate induces a chaotic dynamics for any multipolarity, independently of the geometry of the billiard. If the coupling terms are switched off, the “wall formula” predictions are recovered. We discuss the dissipative behavior of the wall motion and its relation to the order-to-chaos transition in the dynamics of the microscopic degrees of freedom. [S0556-2813(98)03911-9]

PACS number(s): 24.60.Lz, 21.10.Re

I. INTRODUCTION

In the last 20 years the dissipation of collective motion in nuclei has been widely observed [1] in low energy particle and heavy ion collisions and it still represents a theoretically unsolved problem. It is commonly believed that both one-body processes, i.e., collisions of nucleons with the nuclear wall generated by the common self-consistent mean field, and two-body collisions produce dissipation, although their interplay is not well known [2,3].

The theory of damping and the approach to the equilibrium of a collective (usually slow) degree of freedom coupled to noncollective (usually fast) degrees of freedom is a quite general one, both at classical and quantal levels. In the last decades several papers have been published on the subject; see, for example, Refs. [4–16]. The most studied case is the extreme adiabatic limit, namely, when the ratio between the characteristic times of the fast degrees of freedom and of the slow one is considered arbitrary small. Under the further assumption that the fast degrees of freedom have an ergodic dynamics for a fixed value of the collective variable, a description of the damping and approach to quasi-equilibrium can be given in terms of generalized diffusion equations [4,5]. The theoretical framework for the treatment of this limiting case, at least at the classical level, seems to be well established, despite some questions appearing to be still open [6]. Unfortunately, in the majority of realistic cases the adiabatic condition is only partly satisfied and the ergodic condition is not often fulfilled. The damping, however, is still necessarily connected to some degree of chaoticity of the overall dynamics of the system. The connection between chaotic dynamics and dissipation in this more general situation has been studied by different authors but still lacks a general theoretical framework. In particular Wilkinson [4] presented some evidence which indicates that the occurrence of an integrable or nearly integrable motion of the fast degrees of freedom strongly suppresses both the fluctuations and the speed of relaxation towards equilibrium. Related

studies have been developed in Ref. [17], where a coexistence of chaoticity and slow relaxation to equilibrium in a Hamiltonian mean field (HMF) model has been found, and in Ref. [18], where the relation between chaoticity and the approach to equilibrium in a hard sphere gas and a Lorentz gas has been analyzed.

In this context, Blocki *et al.* [11] analyzed the behavior of a gas of classical noninteracting particles enclosed in a multipole-deformed container which undergoes periodic shape oscillations. Particles move on linear trajectories and collide elastically against the walls. In this model the wall and particle motions are uncoupled and therefore the wall keeps oscillating at the same frequency pumping energy into the gas. For this system, the authors study the increase of the particle kinetic energy as a function of time. They find that for octupole and higher modes the gas kinetic energy increases with time, in agreement with the “wall formula” predictions [10]. They attribute the different behavior to the fact that for low multipolarity deformation the particle motion is regular and corresponds to an integrable situation, whereas for higher multipolarities shape irregularities lead to a divergence between trajectories and therefore to chaotic motion. Although their results look very interesting, their application to nuclear or similar cases is not straightforward because (i) the self-consistent mean field is absent and (ii) the total energy is not conserved.

A step forward in this direction has been performed by Bauer *et al.* in Ref. [15]. In this work the authors study the damping of collective motion in nuclei within the semiclassical Vlasov equation. Here self-consistency is taken into account and the total energy is conserved. A multipole-multipole interaction of the Bohr-Mottelson type is adopted for quadrupole and octupole deformation. In both cases dynamical evolution shows a regular undamped collective motion which coexists with a weakly chaotic single-particle dynamics.

In Ref. [16] we introduced a simple model which can shed light on the correlation between chaoticity and dissipa-

tion. We considered a gas of classical noninteracting particles moving in a two-dimensional billiard with nuclear dimensions. Particles collide with the oscillating walls and transfer energy to it, but the container can give back this energy, heating the gas. We considered the gas + billiard as a Hamiltonian system; therefore the total energy is conserved with a good accuracy. Though no explicit dissipative term is considered, the main effect of the coupling of the wall with the particles is a damping of the collective motion. The particle-wall coupling considered in our model is relevant for at least two other reasons: (i) the coupling can enhance the collectivity of the motion, since the particles are indirectly coupled among each other through the wall, and (ii) only with coupling included can the motion of the particles be driven to equilibrium at large time scales. In fact, it has been shown [12] that without the coupling the asymptotic particle velocity distribution is non-Maxwellian.

In Ref. [16] only the monopole case was considered together with a small number of particles, namely, 1 and 10. Here we extend the previous study by considering more particles ($N=30$) and $L=2,3$ multipolarities. For a fixed value of the wall deformation, the motion of the particles is regular in the case of the monopole, $L=0$, partly chaotic for large deformation in the quadrupole case $L=2$, and essentially chaotic in the octupole case $L=3$. In this way we are exploring a set of physical conditions for which the motion of the fast degrees of freedom ranges from nearly ergodic to integrable (for a fixed value of the slow variable). The parameters of the model are chosen as typical at nuclear scales. However, the considered set of dynamical systems should be generic enough to be representative of the physical problem under study, namely, the damping process of a slow degrees of freedom in a bath of many fast degrees of freedom, far enough from adiabaticity and for different degrees of ergodicity. We therefore expect that the results we have obtained are generic enough to be qualitatively valid for a wide class of physical systems.

The most important findings of our study are that (a) chaos shows up in the single-particle motion for any surface deformation for long time scales, (b) the different geometry influences only the time scale for the onset of chaoticity which is faster for the higher multipolarities, (c) the different time scales for the onset of chaoticity are in any case equal within a factor of 2, (d) the dissipation of the collective motion is sensitive only to this time scale and thus it depends only slightly on the geometry of the billiard for $L=2$ and $L=3$, and (e) though no explicit dissipative term is considered in our model, the damping of the collective motion is in practice irreversible due to the large Poincaré time.

The present paper is organized as follows. We summarize the details of the model in Sec. II. The numerical results are illustrated in Sec. III. Conclusions are drawn in Sec. IV.

II. MODEL

In Ref. [16] we considered a classical version of the vibrating potential model (see, e.g., Ref. [19]). In this model several noninteracting classical particles move in a two-dimensional deep potential well and hit the oscillating surface. Using polar coordinates, the Hamiltonian depends on a set of $\{r_i, \theta_i\}$ variables, describing the motion of the par-

ticles, and the collective coordinate α . The Hamiltonian reads

$$H(r_i, \theta_i, \alpha) = \sum_{i=1}^N \left(\frac{p_{r_i}^2}{2m} + \frac{p_{\theta_i}^2}{2mr_i^2} + V(r_i, R(\theta_i)) \right) + \frac{p_\alpha^2}{2M} + \frac{1}{2}M\Omega^2\alpha^2, \quad (1)$$

where $\{p_{r_i}, p_{\theta_i}, p_\alpha\}$ are the conjugate momenta of $\{r_i, \theta_i, \alpha\}$. $m=938$ MeV is the nucleon mass, and $M=\eta mNR_0^2$ is the Inglis mass, chosen proportional to the total number of particles N and to the square of the circular billiard radius R_0 . The value of the factor η is fixed in such a way to minimize the equilibrium fluctuations. In our case $\eta=1$ for the monopole oscillation, whereas $\eta=10$ for quadrupole and octupole. Therefore, in the $L=0$ case, collisions of particles against the walls are more inelastic. Ω is the oscillation frequency of the collective variable α . The potential $V(r, R(\theta))$ is zero inside the billiard and a very steeply rising function on the surface,

$$V(r, R(\theta)) = \frac{V_0}{1 + \exp\{[R(\theta) - r]/a\}},$$

with $V_0=1500$ MeV and $a=0.01$ fm. Such a small value of the diffuseness was chosen in order to simulate closely a billiard system. Larger values of a should not affect qualitatively the results. The surface is described by $R(\theta)=R_0[1 + \alpha \cos(L\theta)]$. Therefore this potential couples the collective variable motion to the particle dynamics and prevents particles from escaping. The numerical simulation is based on the Hamilton's equations

$$\dot{r}_i = \frac{p_{r_i}}{m}, \quad \dot{p}_{r_i} = \frac{p_{\theta_i}^2}{mr_i^3} - \frac{\partial V}{\partial r_i}, \quad (2)$$

$$\dot{\theta}_i = \frac{p_{\theta_i}}{mr_i^2}, \quad \dot{p}_{\theta_i} = -\frac{\partial V}{\partial R} \frac{\partial R}{\partial \theta_i}, \quad (3)$$

$$\dot{\alpha} = \frac{p_\alpha}{M}, \quad \dot{p}_\alpha = -M\Omega^2\alpha - \sum_i \left(\frac{\partial V}{\partial R_i} \frac{\partial R_i}{\partial \alpha} \right). \quad (4)$$

Note that dropping the V term in the equation for p_α , the wall motion becomes purely harmonic and decoupled by the particle motion, as assumed in the model proposed by the authors of Refs. [11,10].

We solve Hamilton's equations with an algorithm of fourth-order Runge-Kutta type with typical time step sizes of 1 fm/c. If not otherwise stated, the calculations were performed with the number of particles $N=30$. The total energy was conserved with relative error $\Delta E/E \leq 10^{-4}$. For runs with the longest time duration or with the largest number of particles a fourth-order symplectic integrator [20] was used, since it turns out to be more efficient with comparable degree of accuracy.

As far as the initial conditions are concerned, we assign random positions to the particles inside the billiard and random initial momenta according to a two-dimensional

Maxwell-Boltzmann distribution with a temperature $T = 36$ MeV. This value of the temperature is chosen in order to mimic the Fermi motion of the particles. In this way the average velocity of the particles is close to the typical nuclear Fermi velocity. In a classical description the use of a Maxwellian distribution ensures that the initial conditions are not too far from equilibrium for the whole system.

We consider the wall oscillations taking place not too far from adiabaticity. For this purpose we follow the definition of the adiabaticity parameter κ given by the authors of Ref. [11], i.e.,

$$\kappa = \frac{\alpha_0 \Omega R_0}{v}, \quad (5)$$

v being the most probable particle speed, $v = \sqrt{T/m}$, α_0 the initial amplitude of the oscillation, and R_0 the radius of the circular billiard. We choose $R_0 = 6$ fm and $\Omega = 0.05$ s⁻¹ so that

$$\kappa = 1.53\alpha_0. \quad (6)$$

With our choice of α_0 (see below), the adiabaticity parameter κ might be not as small as assumed in the asymptotic theory of Ref. [4,5]. The adopted value can correspond more to realistic situations.

Since in realistic cases the collective motion takes place around equilibrium, the initial wall coordinate has been chosen equal to $\alpha_0 = \bar{\alpha} + \delta\alpha$, where $\bar{\alpha}$ is the equilibrium value and $\delta\alpha$ the deviation. The equilibrium value $\bar{\alpha}$ corresponds of course to the thermodynamic limit, which is actually reached when considering an ensemble of copies of the system, all of them with an initial value $\alpha = \bar{\alpha}$ and differing from each other in the initial microscopic distribution of particle positions and momenta. The equilibrium value depends on the considered multipolarity. In all cases we checked numerically that starting from the thermodynamical value $\alpha = \bar{\alpha}$ and a Maxwell-Boltzmann distribution, the collective variable α oscillates in time around $\bar{\alpha}$. Furthermore, we considered an ensemble of this type of run, each one corresponding to different particle initial conditions, consistent with a space uniform distribution and a Maxwell-Boltzmann velocity distribution. We then checked that the average over the runs of the value of collective variable $\alpha(t)$, at any given time t , was converging indeed to the constant equilibrium value $\bar{\alpha}$ for a reasonably large number of runs. In this way one can also estimate the fluctuations around equilibrium the variable α undergoes in a typical run. Also the average amplitude of the fluctuations turns out to be consistent with the thermodynamical estimate for a harmonic oscillator in a thermal bath. More details on the procedure can be found in Ref. [16]. After we checked that the numerical simulation produces good equilibrium properties, we perturbed the equilibrium collective coordinate $\bar{\alpha}$ by an amount $\delta\alpha = 0.3$, and let both the billiard and the particles evolve in time. The chosen value is larger by about a factor of 3 than the average equilibrium fluctuations. Moreover, at time $t=0$ we put $p_\alpha = 0$, the wall having only potential energy.

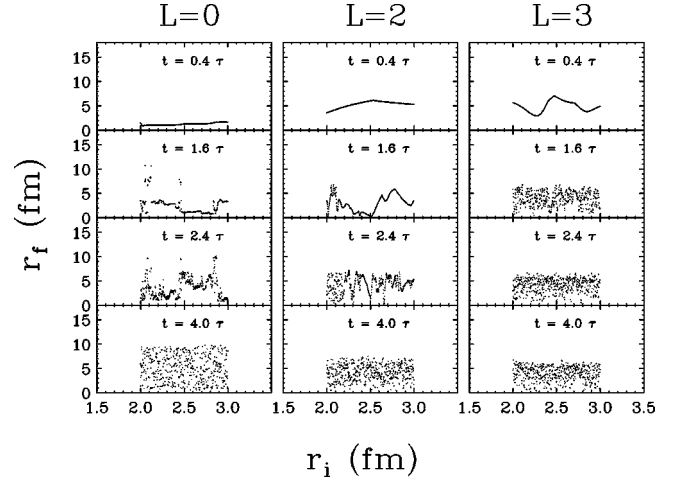


FIG. 1. The final radial coordinate for one particle is drawn as a function of the initial one at different times $t = 0.4\tau$, 1.6τ , 2.4τ , and 4τ . Calculations are performed for multipolarities $L = 0, 2, 3$. Here 1000 initial conditions are considered.

III. NUMERICAL RESULTS

A. Scatter plots

One possible way in order to investigate the role played by the coupling and see whether it can induce chaotic dynamics is drawing Poincaré's surface of sections for the single-particle coordinate. However, this is impossible to perform in our case because of the large number of degrees of freedom. Then an alternative way to visualize a chaotic behavior is to draw scatter plots; see Fig. 1. There we display the final radial coordinate at a time t of one particle vs the one at $t=0$ for the monopole, quadrupole, and octupole deformation. The chosen times are $t = 0.4\tau$, 1.6τ , 2.4τ , and 4τ , τ being the period of the oscillation, $\tau = 2\pi/\Omega$. These plots are very useful and are commonly used in transient irregular situations like chaotic scattering [21] and nuclear multifragmentation [22]. The idea is that if the dynamics is regular, two initially close points in space stay close even at later times, but if the dynamics is chaotic, the two points will soon separate due to the exponential divergence induced by chaos. In the first case this plot will show a regular curve, whereas in the other one a diffused pattern appears. We note that for all multipolarities the initially regular curves change into scattered dots, which clearly show that the coupling to the wall oscillation randomizes the single-particle motion. This is at variance with what was discussed in Ref. [11], where chaos is supposed to appear only for multipolarities $L > 2$. In our model the coupling between the wall and particle motions produces a chaotic dynamics even for $L \leq 2$. In addition, the higher the multipolarity, the earlier chaos starts because of the increased shape irregularity.

A more quantitative analysis can be performed because scatter plots of Fig. 1 have a typical fractal structure. As already done in Ref. [22], a fractal correlation dimension D_2 can be calculated from the correlation integral $C(r)$ [23]. One first counts how many points have a smaller distance than some given distance r . As r varies, so does the correlation integral $C(r)$, defined as

$$C(r) = \frac{1}{M^2} \sum_{i,j}^M \Theta(r - |\mathbf{z}_i - \mathbf{z}_j|), \quad (7)$$

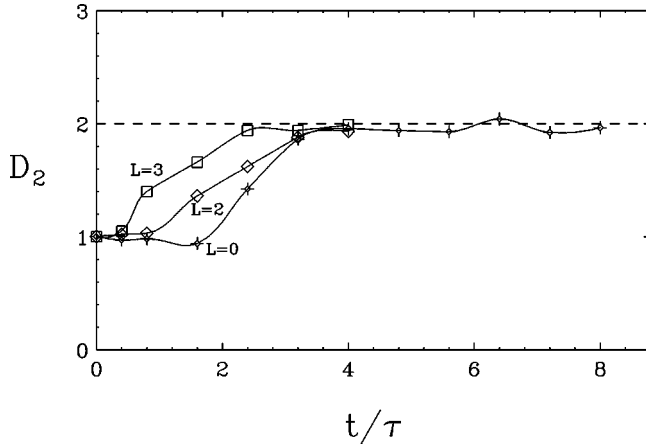


FIG. 2. The time evolution of the fractal correlation dimension D_2 is plotted for the multiplicities $L=0, 2, 3$. The lines are a guide to the eye. The dashed line is the fully random limit for scattered points on a plane.

where Θ is the Heaviside step function and \mathbf{z}_i a vector whose two components (x_i, y_i) are the points coordinates. M is the total number of points. The fractal correlation dimension D_2 is then defined by

$$D_2 = \lim_{r \rightarrow 0} \frac{\ln C(r)}{\ln r}. \quad (8)$$

Therefore by plotting the logarithms it is possible to extract D_2 by fitting the linear slope for sufficiently small r . We considered as a good interval satisfying Eq. (8) the one between $r_{\min} = 1.83 \times 10^{-2}$ and $r_{\max} = 1$. An ensemble of 1000 points was considered. In Fig. 2 we display D_2 vs time for each multiplicity. At the very beginning D_2 is equal to 1, showing that the motion is regular. As time goes on, regularity is lost and the motion becomes chaotic until a complete randomness is reached, in which case $D_2 = 2$ as expected for a completely random distribution on the plane [22]. This result confirms the one published in Ref. [16], where a different method of calculation was, however, employed.

B. Lyapunov exponents

A more common quantitative way to characterize the dynamics in a chaotic regime is by means of the largest Lyapunov exponent λ_1 , which gives the average rate of exponential divergence of two trajectories with nearly identical initial conditions. In general, if we denote by $d(t)$ the distance between two phase space trajectories and $d_0 = d(0)$, λ_1 characterizes the average growth of the distance $d(t)$ with time

$$\langle d(t) \rangle = d_0 \exp(\lambda_1 t). \quad (9)$$

We have calculated this largest Lyapunov exponent λ_1 by the method of Benettin *et al.* [24]. This method consists of evolving two close trajectories originally separated in phase space by d_0 , for a given time interval τ , after which the magnitude of their separation $d(\tau)$ is rescaled back to d_0 . The procedure is then repeated k times. It can be shown that λ_1 is given by the following limiting procedure:

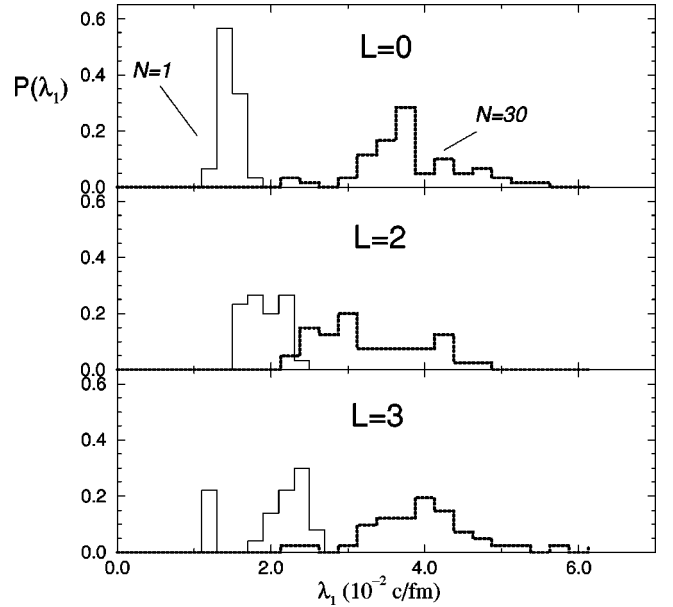


FIG. 3. For the cases $L=0, 2, 3$ we show the frequency distributions of the largest Lyapunov exponent λ_1 for 1 (thin histogram) and 30 particles (thick histogram). An ensemble of about 40 events was considered in each case.

$$\lambda_1 = \lim_{k \rightarrow \infty} \lim_{d_0 \rightarrow 0} \frac{1}{k\tau} \sum_{i=1}^k \ln \frac{d_i(\tau)}{d_0}. \quad (10)$$

The result turns out to be essentially independent of d_0 . We considered the following metric in phase space:

$$d(t) = \sqrt{\sum_{j=1}^N (\delta x_j^2 + \delta p_{x_j}^2 + \delta \theta_j^2 + \delta p_{\theta_j}^2)}, \quad (11)$$

where the infinitesimal distances were normalized to the mean values and therefore are dimensionless quantities. In our case the length of the time interval τ was 200 fm/c and $d_0 \approx 2 \times 10^{-6}$. Using the above method, a large number of trajectories (of the order of 40) was sampled for each multiplicity. Each trajectory was followed for a time $t = 3500$ fm/c, thus allowing for a safe determination of the largest Lyapunov exponent.

In Fig. 3 we display for each multiplicity a distribution of λ_1 for a number of trajectories and for 1 and 30 particles (respectively, thin and thick histograms). The most probable values do not depend strongly on the multiplicity, at variance with the results found in Ref. [11], and lie within a factor of 2 one from each other, the case $L=0$ being intermediate between $L=2$ and $L=3$. This is probably due to the different choice of the wall mass. In the case $N=1$, λ_1 is always smaller than the value obtained with $N=30$, thus showing that (a) chaos starts earlier when a higher number of particles is present and (b) for long time scales the degree of chaoticity is more dependent on the number of particles than on the multiplicity. Therefore a Hamiltonian with coupling terms gives rise to a dynamics weakly dependent on the geometry of the billiard. It has to be noticed that the average number of particle-wall collisions per oscillation period is only about 2 for $N=1$ and about 60 for $N=30$.

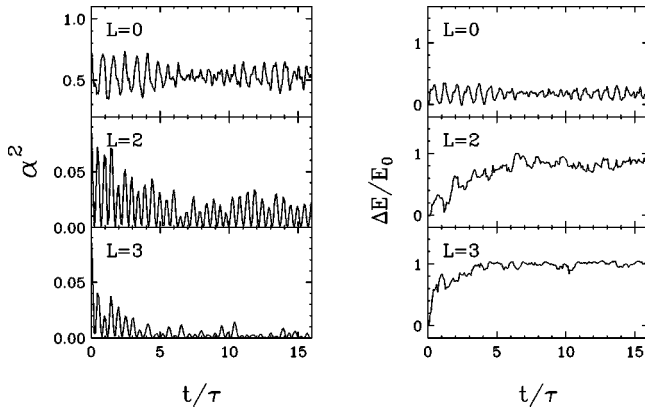


FIG. 4. On the left-hand side the time evolution of the collective variable is shown for the multiplicities $L=0, 2, 3$ and on the right-hand side the corresponding excitation energy of the gas, normalized to the initial energy E_0 .

C. Chaos and dissipation

1. Analysis of the single event

In this section we will mainly discuss the interplay between chaoticity of the single-particle dynamics and dissipation of the collective motion. For this purpose, we follow at the same time the dynamics of the wall and the particles.

First we analyze the behavior of one single event, keeping in mind that a correct statistical description can be performed only for an ensemble of events, as already pointed out in [16]. On the left-hand side of Fig. 4 we plot the evolution of the square of the collective variable α^2 vs time for one single event. Each panel corresponds to a fixed multipolarity. We note that the amplitude of the collective motion shows an irregular oscillation, at variance with the results found in Ref. [15]. We note also that a slight damping can be observed, in contrast with the results published in Ref. [16], where calculations with a smaller number of particles were performed. Please note that α keeps on oscillating around the equilibrium value $\bar{\alpha}$ which for the monopole case depends on the gas temperature and on the wall frequency [16]. For the other multiplicities α oscillates around zero and α^2 decreases more rapidly for increasing L , indicating a faster dissipation for a larger irregularity of the billiard.

On the right-hand side of Fig. 4 we plot the time evolution of the excitation energy of the gas, defined as the relative variation of the total energy of the gas E with respect to its initial value E_0 , $\Delta E/E_0$. In all three cases the gas is heated up, but with a different time dependence according to the multipolarity. Except for small irregular fluctuations, an increasing trend shows up for the quadrupole and octupole modes. An oscillating pattern, slightly irregular, is visible for the monopole case. Moreover, in the $L=0$ oscillation the energy gained by the gas is lower than in the $L=2,3$ cases. Therefore some dissipation is present for all multiplicities and is larger for increasing L . Of course these are only general features of the events for different multiplicities, the details being different from one event to the other.

In order to better understand the mechanism of dissipation, we display in Fig. 5 the square of the ratio α/α_0 , being $\alpha_0 = \alpha(t=0)$. The plot is as function of time, for different multiplicities L and particle number N . In our model the

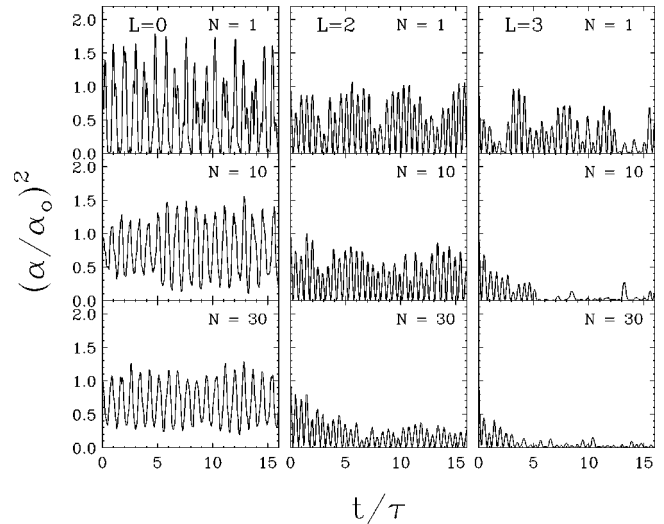


FIG. 5. The square of the ratio α/α_0 is plotted vs the number of oscillations for different multiplicities and number of particles.

total energy is conserved so that the damping of the wall motion corresponds to the heating of the gas. This process is in principle reversible, but the high number of degrees of freedom involved makes in practice this process irreversible. One should wait a very long time, i.e., the Poincaré time, to see the system again close to the initial conditions. We note that the dissipation is stronger when both L and N increase. In particular, the increased number of particles makes the available phase space bigger and the Poincaré time longer. The latter can therefore be a limitation, in the sense that a short Poincaré time would weaken dissipation.

2. Analysis of an ensemble of events

In order to have a global picture of the macroscopic system, many events are needed and average values of the different observables should be considered. In Fig. 6 we display the time evolution of α^2 averaged over an ensemble of 1000 different events, each obtained by assigning random initial

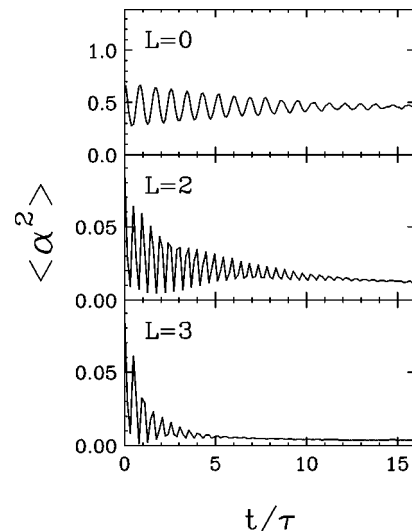


FIG. 6. The square of the collective variable α , averaged over an ensemble of 1000 events, is displayed vs the number of oscillations for the three multiplicities considered.

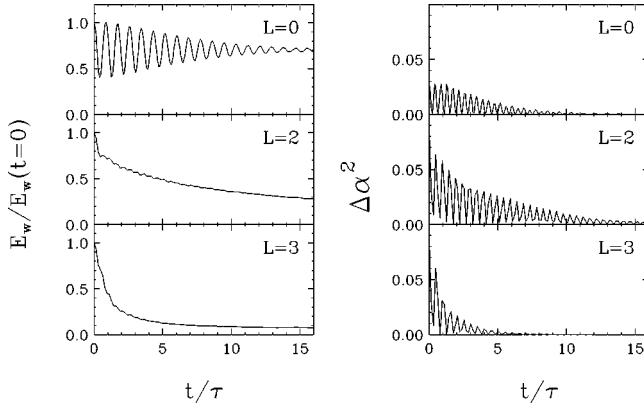


FIG. 7. On the left-hand side the wall energy, averaged over an ensemble of 1000 events and normalized by its initial value, is reported vs the number of oscillations for different multiplicities. On the right-hand side the observable $\Delta\alpha^2$ is drawn (see text for further details).

conditions to the particles both in coordinate and momentum space but consistent with a Maxwellian. We note that the motion of the collective variable $\langle\alpha^2\rangle$ is completely damped out for times which depend on the multipolarity and develops around equilibrium, as we checked explicitly. The reader should keep in mind that for $L=0$ collisions of the particles with the wall are more inelastic (see Sec. II) due to the lighter mass of the wall; therefore the monopole oscillation damps out in a time comparable with the one of the $L=2$ mode. The same mass was used in the calculations published in Ref. [16]. If we put $\eta=10$ even for $L=0$, the damping time is longer.

The damping of the oscillations, which is apparent in Fig. 6 for all the three multiplicities, can have two distinct origins. On the one hand, each individual event can indeed display a damping of the oscillation amplitude. In this case the effect of the average is only of a smoothing the fluctuations. The observed damping time is then simply the average damping time of a generic set of events. On the other hand, each event has a different time evolution, and after a period of time the *phase* of the oscillation can be quite different from one event to another. If the phase becomes essentially random as the time proceeds, when taking the average of α over different events strong cancellations can occur and a damping of the oscillations can appear, even in the case where no average energy damping is present. It is worth noticing that this damping mechanism disappears if the ratio between the single-particle mass and the wall mass is vanishing small, and therefore it is ineffective at the macroscopic level, where event-to-event fluctuations can be neglected. In order to estimate the contribution of each one of the two mechanisms to the damping displayed in Fig. 6, we plot on the left-hand side of Fig. 7 the energy of the wall divided by its initial value, averaged over the same sets of events. As a function of time, this quantity should be insensitive to phase randomization because it is proportional to $\langle\alpha^2\rangle$ and corresponds to the average energy damping of the oscillations.

For comparison, on the right-hand side we plot also $\Delta\alpha^2 = (\langle\alpha\rangle - \alpha_\infty)^2$, a quantity which, on the contrary, should be sensitive to phase cancellations. For the monopole case,

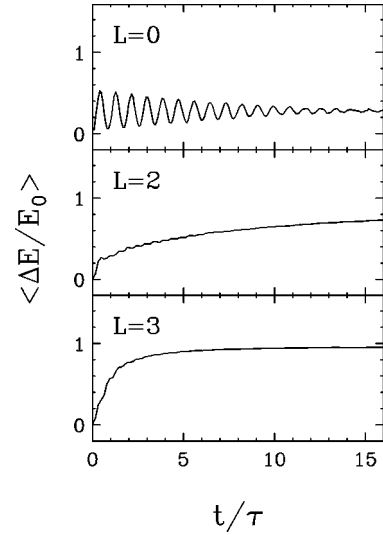


FIG. 8. The excitation energy of the gas, averaged over an ensemble of 1000 events, is reported vs the number of oscillations for different multiplicities.

the decay time of the wall energy to its asymptotic value α_∞ is substantially longer than the one for $\Delta\alpha^2$, which indicates that for the monopole case the dephasing mechanism is quite important. The asymptotic value of $\langle\alpha\rangle$ is consistent with the equilibrium value $\bar{\alpha}$ for a gas at the final temperature, which, from energy conservation, turns out to be $T=43$ MeV. We checked that indeed the velocity distribution, averaged over the events, is very close to a Maxwellian with that temperature. Furthermore, the average amplitude of the fluctuations around the equilibrium value was checked to be consistent with a harmonic oscillator in equilibrium with a thermal bath at $T=43$ MeV.

On the contrary, for the higher multiplicities the decay times of the wall energy and $\Delta\alpha^2$ appear to be very close, and therefore the dephasing mechanism seems to be in these cases ineffective. The damping is mainly an energy damping and is characteristic of a generic event.

These considerations are confirmed if one calculates the excitation energy of the gas, displayed in Fig. 8. We note that the characteristic times for the energy growing follow closely in all cases the decay times of the wall energy. Moreover, for $L=2,3$ we note the presence of two different regimes: a first one lasting for about one to two oscillations characterized by a sharp rise in the excitation energy, and a second one at successive times where a slower approach to equilibrium is apparent. As can be deduced from Fig. 1, the first stage may have some relation with the onset of chaos in the single-particle motion. After chaos has fully developed, and an appreciable part of the total energy has been pumped into the gas, a certain degree of randomization is reached and a slower dissipation rate shows up. A similar behavior in the relaxation was observed for the HMF model [17] and the hard sphere gas and the Lorentz gas studied in Ref. [18]. In the latter cases the time evolution of the Boltzmann entropy was studied.

This behavior is completely absent in the monopole case. Therefore it seems that different kinds of dissipation can originate from the same underlying chaotic single-particle motion. It should be stressed that, within the time of chaos

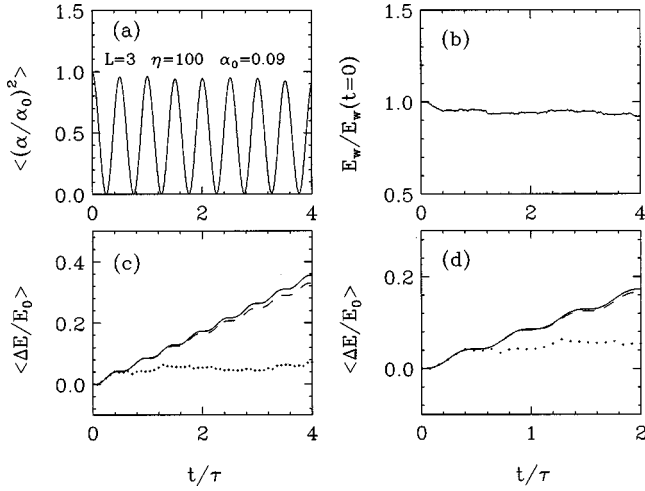


FIG. 9. Coupled octupole motion of the wall and gas particles with a very large inertia of the wall ($\eta=100$). The adiabaticity parameter is $\kappa=0.14$. Shown are the time evolutions of the collective variable [panel (a)] and the wall energy [panel (b)] according to our model (solid line). The relative increase of the gas energy is shown as dots in comparison with two different versions of the wall formula (solid and dashed lines) as explained in the text [panel (c)]. Panel (d) is a blow-up of panel (c).

development, the wall has dissipated only a fraction of its energy, as is clearly seen in Fig. 7. In the monopole case it is apparent that the flow of energy from the collective variable α to the particle gas is not completely “irreversible,” and the wall receives back part of its energy from the gas for a number of oscillations.

3. Comparison with the wall formula

Let us now try to make some connection to one-body dissipation and the wall formula introduced and studied extensively in the past by Blocki *et al.* [11,10]. We limit ourselves to the analysis of the octupole mode, because for that (and for higher multiplicities) the model of Blocki *et al.* predicts dissipation. Of course a comparison between the situation studied here and in [11] may be biased because in the model studied in [11] there is no energy conservation. Therefore the phase space of the gas is conserved in the latter model but not in the case considered here. In spite of that our model should be able to recover the limit of Blocki *et al.* And actually it does. This happens when in our model the mass of the wall becomes very large as, for example, in Fig. 9 where we choose $\eta=100$ and $\alpha_0=0.09$ with $N=30$ and $\Omega=0.05$ as before. In this case the particle-wall collisions are more elastic and the time evolution is slower for all observables. In particular in panels (c), (d) of Fig. 9 the dots are our numerical simulation and the solid and dashed lines are two versions of the wall formula to be explained in the Appendix. In particular, the dashed line represents the results of the wall formula which contains only terms linear in time. The inclusion of terms quadratic in time, which take into account the increased average speed of the gas for large times, produces a new dissipation formula represented in Figs. 9 and 10 by a solid line. Now, if every thing is consistent we should get the same result as the one shown in Fig. 9 in switching off the

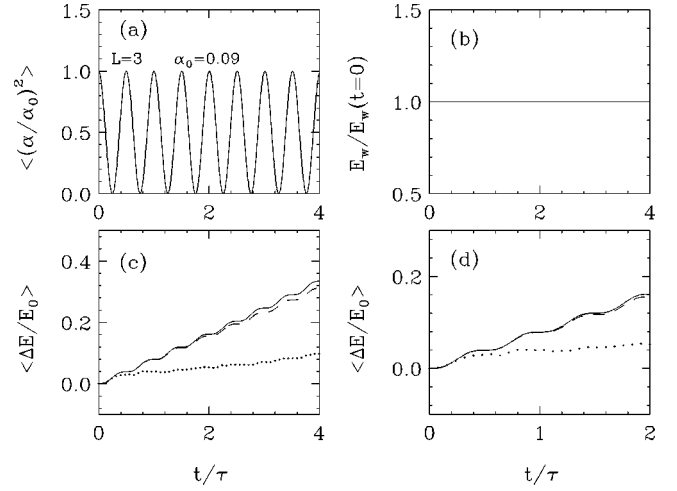


FIG. 10. Same as Fig. 9 but without coupling. The frequency of the wall is kept fixed to the initial one, i.e., $\Omega=0.05 \text{ s}^{-1}$.

coupling. That this is actually the case is shown in Fig. 10 where the time evolution of the different quantities is practically the same as in Fig. 9.

A particular feature of the case shown in Figs. 9 and 10 is the fact that the wall formula results follow the exact evolution only during the first period. We should emphasize that we applied here the wall formula adapted to the two-dimensional case, as derived in the Appendix. In Fig. 11 we show a repetition of the calculation in Ref. [11] where the wall formula follows the exact result for the heating of the particles gas over several periods. The only difference with the calculation in [11] is that here we use again for the gas particles our Maxwell-Boltzmann distribution with $T=36 \text{ MeV}$, whereas in [11] a sharp Fermi-Dirac distribution was employed. The fact that the wall formula for this particular case of the parameters is well reproduced indicates that this feature is independent of Maxwell-Boltzmann or Fermi-Dirac statistics. This must be expected, since in the wall formula the dissipation rate depends only on the average velocity of the particles. Therefore, the dissipation must be

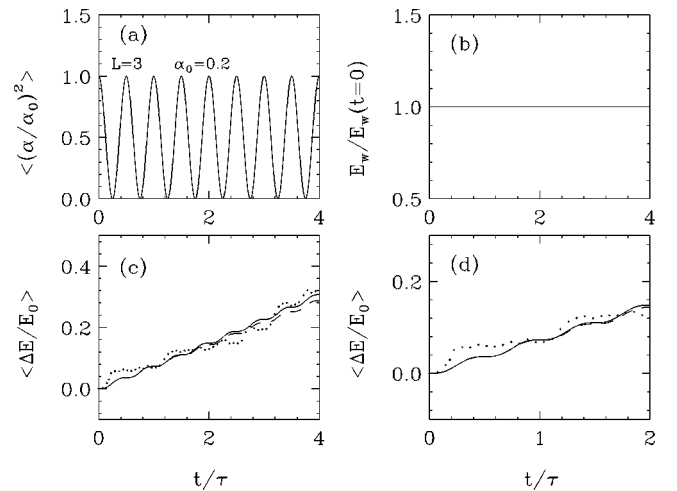


FIG. 11. Repetition of the calculation of Blocki *et al.* [11], but with a Maxwellian distribution for the gas particles. The observables displayed are the same as in Figs. 9 and 10. The adiabaticity parameter is $\kappa=0.04$. See the text for more details.

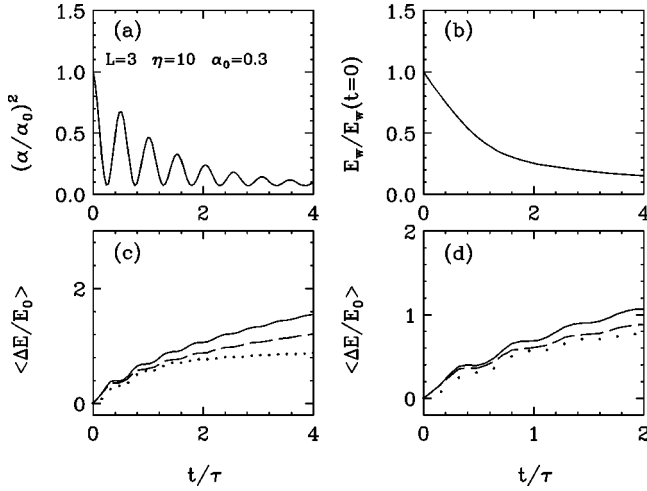


FIG. 12. Same as Fig. 9 with coupling. In panels (c) and (d) time-dependent wall formulas have been used, taking into account, respectively, terms linear in time (dashed line) with quadratic ones (solid line). The dots are our numerical results.

the same as long as the average velocity of the particles is the same. The only variance with the case shown in Figs. 9 and 10 is that the parameters are slightly different, for instance, the adiabaticity parameter κ defined in Eq. (6) is by almost a factor of 4 smaller in Fig. 11 than in Figs. 9 and 10, that is, $\kappa=0.04$ instead of $\kappa=0.14$. However, both values of κ are sufficiently small in order to verify the adiabaticity criterion (for the validity of the wall formula) established by Blocki *et al.*, namely, that $\kappa \ll 1$. According to our findings here, κ must really be extremely small so that the wall formula holds during several periods; otherwise it may be valid only during the first instances of the dynamics.

Let us now come back to a more detailed analysis of our present results obtained including the coupling terms in the Hamiltonian. In Fig. 12 we show as a function of time the evolution of the elongation [panel (a)], the wall energy [panel (b)], and the gain in energy of the gas [panel (c)] together with a blowup of (c) [panel (d)]. In panels (c) and (d) are also shown the results of the standard wall formula (dashed line), which is linear in time [11], and the new version including a quadratic term (solid line) [12]. We should stress that we applied here generalized wall formulas, taking account of the fact that the wall motion is actually damped. This implies that we have to use a time-dependent version of the wall formula (TDWF) as derived in the Appendix.

Again we see that the wall formula only agrees with the exact solution during the first period. For longer times the wall formulas give rise to much more energy dissipation than in the exact evolution, the new formula more than the standard one.

From the above investigations it seems therefore that the wall formula can only simulate the dissipation of energy in the first instances of the dynamics when the adiabaticity parameter κ [Eq. (6)] is extremely small (of the order of 1/100).

IV. CONCLUSIONS

In conclusion, we have presented a dynamical approach based on the solution of the Hamilton's equations for several

particles moving in a classical billiard having nuclearlike dimensions, in order to explain dissipation of the collective motion. We found that the presence of a coupling term in the single-particle Hamiltonian induces chaotic motion at the microscopic level.

As far as the monopole mode is concerned, we found irregular behavior together with damping in single events. The damping observed when an average is taken over a set of events is a consequence also of the irregular time dependence of the oscillations. This incoherence is produced by the chaotic single-particle dynamics, which makes all events belonging to the same ensemble different one from each other, and therefore substantial cancellations occur once the average is taken. For the higher multipolarities this mechanism seems to be ineffective, and the damping coincides with a real energy damping of the oscillations due to the large Poincaré time. The dissipative process for the quadrupole and octupole modes looks different also in another respect. In fact, while the single-event properties are similar to the monopole case, an ensemble of events shows that two different regimes appear: (a) an initial fast dissipative evolution corresponding to the onset of chaos in the single-particle motion and (b) a slower dissipative trend towards equilibrium.

All these results should be qualitatively independent of the particular nuclear dimensions we have used in the model.

In order to be closer to equilibrium we have used for the initialization of the gas particles a Maxwell-Boltzmann distribution with a temperature of $T=36$ MeV to have a mean kinetic energy characteristic of nuclear systems. We also checked that the use of a Maxwell-Boltzmann distribution versus a Fermi-Dirac step is apparently of no consequence on the damping rate. Indeed in switching off the particle wall coupling and periodically octupole-deforming the wall under the same condition, as was done some time ago by Blocki *et al.* [11] using a Fermi-Dirac step, we find with a Maxwell-Boltzmann distribution an identical rate of feeding of energy into the particle gas. Moreover, we also checked that the wall formula prediction for energy dissipation agrees with the numerical simulation over several periods in time. This shows that our model is able to mock up real nuclear dynamics together with its damping mechanisms.

When we increase the adiabaticity parameter κ by almost a factor of 4 attaining $\kappa=0.14$, which should still be considerable as small, the agreement of the numerical result with the wall formula was reduced to only the first period of the oscillation. In view of what we said above about Maxwell-Boltzmann versus Fermi-Dirac distributions, we assume that this is a generic result. Also when reducing the inertia of the wall by a factor of 10 and thus increasing the particle wall coupling (once reestablished) the heating rate of the particle gas agrees with the wall formula only during the first period. This happens in spite of the fact that we used a time-dependent version of the wall formula where the continuous slowing down of the wall motion has been taken into account. Indeed the wall formula considerably overestimates the damping rate at longer times.

One should realize that our model implies real particle-wall collisions with global energy conservation. Such collisions are absent in pure Hartree-Fock or Vlasov calculations. In fact our model in what concerns the particle wall colli-

sions should come quite close to the situation considered, e.g., in [3] where the collision term is based on the particle vibration coupling model. Also in that model the damping rate strongly differs between low and high multiplicities of the collective motion. However, in Ref. [3], contrary to the spirit of the present work, fast (diabatic) motion (the giant resonances) was considered, which makes a detailed comparison inadequate. In the future, in order to simulate a pure mean field dynamics based on our model, we plan to calculate the evolution with the so-called parallel ensemble technique and ensemble average at each instant of time the motion of the wall. We anticipate that this very much will suppress the particle wall damping mechanism so that the collective oscillation will be mostly undamped, a feature which should bring the present study in closer contact with the one performed in Ref. [15].

Our model certainly has implications beyond nuclear physics. It should be generic for all situations where a heavy particle (here the wall) is moving in a Knudsen gas of light particles. For example the motion of a pendulum of mass M in a very rarefied gas of particles with mass $m \ll M$ should show features similar to the ones studied within the present model. If the big particle can be approximated by a sphere suspended on a spring and the gas is enclosed in a box, the whole system can be considered as some sort of dynamic generalization of a Sinai billiard. The study of the damping of the heavy particle in such a situation would be particularly interesting.

ACKNOWLEDGMENTS

One of us (A.R.) would like to thank Vito Latora, Stefano Ruffo, and Allan Lichtenberg for fruitful discussions.

APPENDIX

Here we give some details about the two-dimensional wall formula. Starting from the original formulation given by Blocki *et al.* in Ref. [10], after rescaling in two dimensions, we get the following result:

$$\frac{dE}{dt} = \frac{4}{\pi} \rho \bar{v} \oint \dot{q}^2 dl + \dots (\text{terms of higher order in } \dot{q}^3). \tag{A1}$$

ρ and \bar{v} are, respectively, the density and the average speed of the gas, \dot{q} is the speed of the wall, and dl is the line element. By integration of Eq. (A1), and neglecting corrections of order α^2 or higher, we easily get

$$\frac{dE}{dt} = 4\rho\bar{v}R_0^3[\dot{\alpha}(t)]^2, \tag{A2}$$

where $\dot{\alpha}(t)$ can be calculated either without or with coupling. In the former case $\alpha(t) = \alpha_0 \cos(\Omega t)$ and Eq. (A2) will read

$$\frac{1}{E_0} \frac{dE}{dt} = \frac{2R_0}{\bar{v}} \Omega^2 \alpha_0^2 \sin^2(\Omega t). \tag{A3}$$

E_0 and α_0 are the initial energy of the gas and the initial elongation. After more algebra we get the excitation energy of the gas, $\Delta E/E_0$:

$$\frac{\Delta E}{E_0} = \frac{R_0}{\bar{v}} \Omega \alpha_0^2 \left[\Omega t - \frac{\sin(2\Omega t)}{2} \right] \text{ no coupling.} \tag{A4}$$

In the case with coupling $\dot{\alpha}(t)$ comes directly from our numerical simulation. In fact, since the wall energy is

$$E_w = \frac{1}{2} M \dot{\alpha}^2 + \frac{1}{2} M \Omega^2 \alpha^2, \tag{A5}$$

we easily get $\dot{\alpha}$ and substitute in Eq. (A2) obtaining

$$\frac{1}{E_0} \frac{dE}{dt} = \frac{R_0}{\bar{v}} \left[\frac{2}{M} E_w - \Omega^2 \alpha^2 \right] \text{ with coupling.} \tag{A6}$$

By integration on time we get again the excitation energy of the gas $\Delta E/E_0$. The last equation is the TDWF.

In Ref. [12], a generalized wall formula has been studied, which takes into account for the increased average speed of the gas for large times. The new dissipation formula contains an additional term quadratic in time, besides the linear term [Eq. (A4)]. We have performed similar calculations in two dimensions, both without and with coupling. The new formula for the excitation energy of the gas reads

$$\frac{\Delta E}{E_0} = 2I(t) + \frac{3}{\pi} I^2(t), \tag{A7}$$

$I(t)$ being, respectively,

$$I(t) = \frac{\alpha^2 \Omega R_0}{2v} \left[\Omega t - \frac{\sin(2\Omega t)}{2} \right] \text{ no coupling,} \tag{A8}$$

$$I(t) = \frac{R_0}{\bar{v}} \int_0^t dt \left[\frac{2}{M} E_w - \Omega^2 \alpha^2 \right] \text{ with coupling.} \tag{A9}$$

[1] J. Speth and A. van der Woude, Rep. Prog. Phys. **44**, 719 (1981).
 [2] A. Smerzi, A. Bonasera, and M. Di Toro, Phys. Rev. C **44**, 1713 (1991), and references therein.
 [3] F. V. De Blasio, W. Cassing, M. Tohyama, P. F. Bortignon,

and R. A. Broglia, Phys. Rev. Lett. **68**, 1663 (1992).
 [4] M. Wilkinson, J. Phys. A **23**, 3603 (1990).
 [5] C. Jarzynski, Phys. Rev. Lett. **74**, 2937 (1995); **71**, 839 (1993).
 [6] M. V. Berry and J. M. Robbins, Proc. R. Soc. London, Ser. A **442**, 641 (1993).

- [7] A. Bulgac, G. Do Dang, and D. Kusnezov, *Phys. Rep.* **264**, 67 (1996), and references therein.
- [8] M. Wilkinson, *J. Phys. A* **21**, 4021 (1988).
- [9] R. Blümel and B. Esser, *Phys. Rev. Lett.* **72**, 3658 (1994); R. Blümel and J. Mehl, *J. Stat. Phys.* **68**, 311 (1992).
- [10] J. Blocki, Y. Boneh, J. R. Nix, J. Randrup, M. Robel, A. J. Sierk, and W. J. Swiatecki, *Ann. Phys. (N.Y.)* **113**, 338 (1978).
- [11] J. Blocki, J. J. Shi, and W. J. Swiatecki, *Nucl. Phys.* **A554**, 387 (1993).
- [12] C. Jarzynski and W. J. Swiatecki, *Nucl. Phys.* **A552**, 1 (1993); J. Blocki, J. Skalski, and W. J. Swiatecki, *ibid.* **A594**, 137 (1995).
- [13] A. Y. Abul-Magd and H. A. Weidenmüller, *Phys. Lett. B* **261**, 207 (1991).
- [14] S. Pal and T. Mukhopadhyay, *Phys. Rev. C* **54**, 1333 (1996).
- [15] W. Bauer, D. McGrew, V. Zelevinsky, and P. Schuck, *Phys. Rev. Lett.* **72**, 3771 (1994).
- [16] G. F. Burgio, M. Baldo, A. Rapisarda, and P. Schuck, *Phys. Rev. C* **52**, 2475 (1995).
- [17] V. Latora, A. Rapisarda, and S. Ruffo, *Phys. Rev. Lett.* **80**, 692 (1998); *Physica D* (to be published), chao-dyn/9803019.
- [18] Ch. Dellago and H. A. Posch, *Phys. Rev. E* **55**, R9 (1997).
- [19] P. Ring and P. Schuck, *The Nuclear Many Body Problem* (Springer-Verlag, Berlin, 1980), p. 388.
- [20] See, for instance, Haruo Yoshida, *Phys. Lett. A* **150**, 262 (1990), and references therein.
- [21] A. Rapisarda and M. Baldo, *Phys. Rev. Lett.* **66**, 2581 (1991); M. Baldo, E. G. Lanza, and A. Rapisarda, *Chaos* **3**, 691 (1993).
- [22] A. Atalmi, M. Baldo, G. F. Burgio, and A. Rapisarda, *Phys. Rev. C* **53**, 2556 (1996).
- [23] P. Grassberger and I. Procaccia, *Phys. Rev. Lett.* **50**, 346 (1983).
- [24] G. Benettin, L. Galgani, and J. M. Strelcyn, *Phys. Rev. A* **14**, 2338 (1976).